THE JOURNAL OF PHYSICAL CHEMISTRY C

Article

Cite This: J. Phys. Chem. C 2018, 122, 8202−8208

pubs.acs.org/JPCC

Excited Spin-State Trapping in Spin Crossover Complexes on Ferroelectric Substrates

Christian Wäckerlin,*[,†,‡] Fabio Donati,[§,†,∥] Aparajita Singha,[†] Romana Baltic,[†] Silvio Decurtins,[⊥] Shi-Xia Liu,[⊥] Stefano Rusponi,[†] and Jan Dreiser*[,#]

[†]Institute of Physics, Ecole Polytechnique Fédérale de Lausanne, Station 3, 1015 Lausanne, Switzerland

[‡]Nanoscale Materials Science, Empa, Swiss Federal Laboratories for Materials Science and Technology, 8600 Dübendorf, Switzerland

[§]Center for Quantum Nanoscience, Institute for Basic Science (IBS), Seoul 03760, Republic of Korea

[∥]Department of Physics, Ewha Womans University, Seoul 03760, Republic of Korea

[⊥]Department of Chemistry and Biochemistry, University of Bern, Freiestrasse 3, 3012 Bern, Switzerland

[#]Swiss Light Source, Paul Scherrer Institut, 5232 Villigen PSI, Switzerland

Supporting Information

ABSTRACT: We have studied thin films of Fe(II) spin crossover complexes deposited on differently poled ferroelectric PMN-PT ($[Pb(Mg_{1/3}Nb_{2/3})O_3]_{1-x}[PbTiO_3]_x$, x = 0.32) substrates by X-ray absorption spectroscopy. The X-ray spectra reveal the temperature-driven conversion between high-spin and low-spin states without any observable effect of the ferroelectric polarization on the spin state of the molecules down to 100 K. In the soft X-ray-induced excited spin-state trapping (SOXIESST) regime at 3 K, large differences occur between the two ferroelectric polarizations. The efficiency of X-rays in exciting the molecules to the high-spin state is more than an order of magnitude larger when the ferroelectric dipoles of the substrate are pointing toward the surface compared to the opposite polarization. We explain our findings by a modulation of the polarization-dependent efficiency of the scattering of X-ray-generated secondary electrons at the molecules. Our results provide a deep insight into the SOXIESST mechanism and suggest that such molecules could be used as detectors for electrons traveling in the substrate at energies lower than the substrate electron affinity.

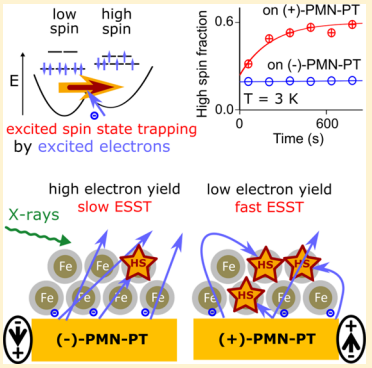

INTRODUCTION

Transition-metal complexes exhibiting thermal spin crossover (SCO) are interesting for fundamental investigations as well as for applications as molecular switches. Thin films of SCO complexes show potential for molecular electronics and spintronics applications, in particular if their crossover can be controlled by external stimuli, such as irradiation by light, interaction with charge carriers, or applied electric fields.[1−3] In SCO complexes, the lowest two electronic states having different spin multiplicities are close in energy. In the case of Fe(II) SCO complexes, the transition occurs between the high-spin (HS) $S = 2$ $^5T_2$ state observed at elevated temperature and the low-spin (LS) $S = 0$ $^1A_1$ state (O_h notation) at low temperature. The transition temperature $T_{1/2}$ is defined as the temperature at which the high-spin (HS) and low-spin (LS) states are equally populated.[4] The fact that complexes in the LS state can be promoted to the HS state by irradiation with light (light-induced excited spin-state trapping, LIESST)[5−8] allows for an additional degree of control. If the temperature T is low enough, then the HS state becomes metastable. In consequence, below T_{LIESST}, the HS state can be observed on exceedingly long time scales. Apart from light, other types of excitation can also result in excited spin-state trapping (ESST). Indeed, ESST has been observed as a consequence of nuclear decay (nuclear decay-induced ESST),[4,9] by excitation with "hot" electrons (electron-induced ESST)[10,11] and by irradiation with ionizing electromagnetic radiation, such as soft X-rays (soft X-ray-induced ESST, SOXIESST),[12,13] hard X-rays (hard X-ray-induced ESST),[14] and vacuum-ultraviolet light (vacuum-ultraviolet light-induced ESST).[15]

Here, we employ X-ray absorption spectroscopy (XAS) at the Fe $L_{2,3}$ edges, which is well suited to determine the electronic ground state of the Fe(II) ion,[16] to study the thermal SCO and the SOXIESST in thin films of SCO molecules on differently polarized ferroelectric substrates. The SCO complex used in this study is $[Fe(H_2B(pz)_2)_2(bipy)]$ (bipy = 2,2′-bipyridine, $H_2B(pz)_2$ = dihydrobis(1-pyrazolyl)borate, cf., scheme in Figure 1a), which is well characterized in the bulk phase.[17] Furthermore, this compound can be deposited by thermal sublimation while keeping its structure intact.[10,18] As a substrate, the ferroelectric PMN-PT ($[Pb(Mg_{1/3}Nb_{2/3})O_3]_{1-x}[PbTiO_3]_x$, x = 0.32) (011) surface is used.[19,20] The ferroelectric can be poled by application of a strong electric field. In consequence, it exhibits a net static electric dipole

Received: November 6, 2017
Revised: March 23, 2018
Published: March 29, 2018

DOI: 10.1021/acs.jpcc.7b10941
J. Phys. Chem. C 2018, 122, 8202−8208

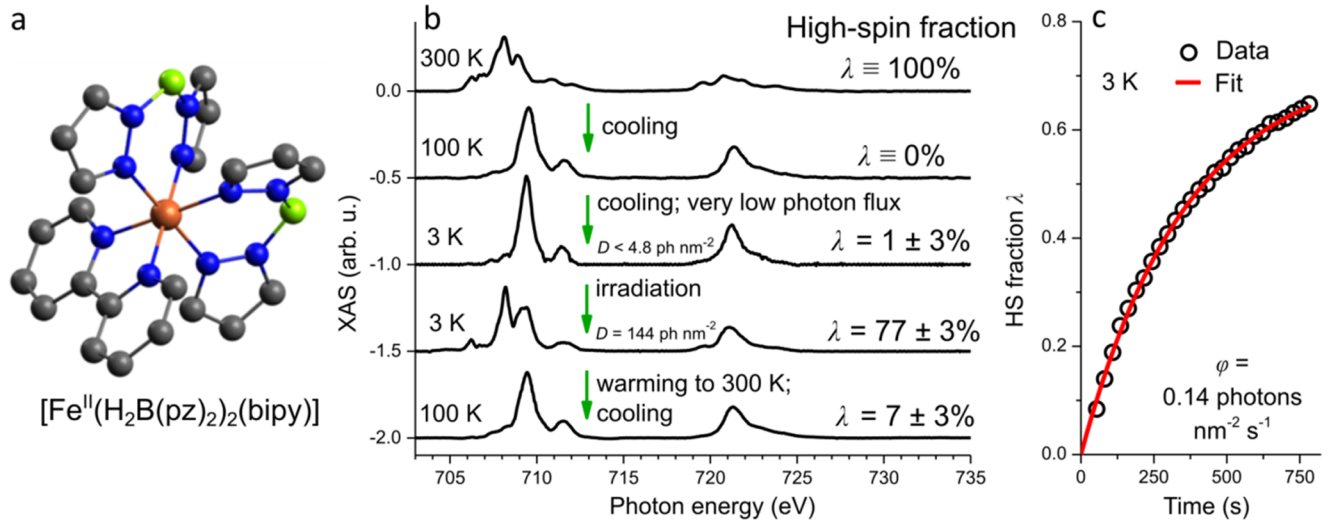

Figure 1. (a) Scheme of the SCO complex $[Fe(H_2B(pz)_2)_2(bipy)]$. Color code: orange, Fe; gray, C; blue, N; green, B. Hydrogen atoms have been omitted for clarity. (b) Sequence of X-ray spectra recorded on a powder sample of $[Fe(H_2B(pz)_2)_2(bipy)]$. The fully reversible high-spin (HS) to low-spin (LS) conversion (300−100 K) and soft X-ray-induced excited spin-state trapping (SOXIESST) at 3 K are visible. Spectra are offset for clarity. (c) Time-dependent HS fraction measured on the powder sample revealing the LS → HS conversion due to SOXIESST at 3 K.

moment pointing toward the surface [(+)-PMN-PT] or toward the back contact [(−)-PMN-PT]. A number of studies report the differences in molecular adsorption/desorption[21−23] and selective suppression of thermal SCO depending on the ferroelectric polarization.[24] However, to the best of our knowledge, no effect of the ferroelectric polarization on SOXIESST has been reported.

EXPERIMENTAL METHODS AND MATERIALS

Synthesis. $[Fe(H_2B(pz)_2)_2(bipy)]$ has been prepared according to literature procedures.[17]

Sample Preparation. The (011)-oriented PMN-PT ($[Pb(Mg_{1/3}Nb_{2/3})O_3]_{1-x}[PbTiO_3]_x$, x = 0.32) substrates (0.5 mm thickness, Atom Optics Co., Ltd., Shanghai, China) were cleaned with acetone and isopropanol. Prior to the deposition of the molecules, the substrates were poled in high vacuum by applying ±320 V between two copper electrodes in direct contact with the front and back surfaces of the chip. The details of the preparation and the characterization of the substrates using X-ray linear dichroism are reported elsewhere.[25,26] The displacement current caused by the switching of the ferroelectric polarization was observed to ascertain that the poling was complete across the whole area of the chip (Figure S1). In case of a negative applied voltage at the back side of the sample, here referred to as "(−)-PMN-PT", the electric dipole moment points toward the surface. For a positive applied voltage at the back side of the sample, here referred to as "(+)-PMN-PT", the electric dipole moment points toward the back contact.

The two thin films of the SCO complex were grown by sublimation of the $[Fe(H_2B(pz)_2)_2(bipy)]$ complexes from a Knudsen cell onto the (+)- and (−)-poled substrates, concurrently in high vacuum while keeping the substrates at ∼10 K to obtain a high sticking coefficient of the molecules. The sublimation temperature was 125 °C, the base pressure was $\sim 10^{-6}$ mbar, and the deposition time was 308 s. The thickness of the obtained films was determined by measuring the step height of an edge produced by masking one part of the sample during the deposition. The average thicknesses of the molecular films were 75 ± 10 and 65 ± 10 nm on (+)- and (−)-polarized PMN-PT, respectively. In between the poling process, the deposition of molecules, and the XAS experiments, the samples were exposed to air. The powder sample was produced by pressing the polycrystalline powder of molecules on an indium foil.

X-ray Absorption Spectroscopy. XAS experiments were performed at the X-Treme beamline[27] (Swiss Light Source, Paul Scherrer Institut) in total electron yield (TEY) mode. The beam was defocused (0.3 × 1.2 mm^2), and spectra were normalized to the TEY measured simultaneously on a gold mesh. The photon (ph) flux was measured at the same fixed energy on the gold mesh, which was referenced to a calibrated photodiode after the last optical element of the beam line.[27] A polynomial background was subtracted from all X-ray spectra shown in this work.

RESULTS AND DISCUSSION

Soft X-ray-Induced Excited Spin-State Trapping in Powder Samples. First, we present the XAS measurements performed on the powder sample, which serves as a reference. The spectra recorded at 300 and 100 K are shown in Figure 1b, above and below the SCO temperature $T_{1/2}$ = 160 K.[17] Consistent with the literature,[16,28,13,29,30] at 300 K, the X-ray absorption spectra exhibit a broad multiplet at the Fe L_3 edge with a peak at 708.2 eV characteristic of the HS state. At 100 K, the Fe L_3 X-ray absorption spectrum is narrow with a peak at 709.5 eV evidencing the LS state. Multiplet calculations reproducing the X-ray absorption spectra of a very similar SCO complex are reported in ref 30.

SOXIESST was studied at 3 K, well below T_{LIESST} = 52 K.[17] At 3 K, the HS → LS relaxation rate is negligible in the time scale of the experiments because even at 10 K the HS state decays only by 4% in 12 h.[31] The spectrum obtained at 3 K (Figure 1b) was recorded with a small X-ray flux of ϕ = 0.04 ph s^{-1} nm^{-2} without prior X-ray illumination at this spot. The recording time of 120 s corresponds to a photon (ph) dose of D = 4.8 ph nm^{-2}. The HS fraction λ = 1 ± 3% was obtained from the relative intensity r of the HS and LS peaks at the Fe L_3 edge, specifically $r = (I_{HS} - I_{LS})/(I_{HS} + I_{LS})$. λ was determined from r by a linear relationship, defining λ = 1 and 0 in the reference spectra obtained at 300 and 100 K, respectively. This

DOI: 10.1021/acs.jpcc.7b10941
J. Phys. Chem. C 2018, 122, 8202−8208

experiment shows that it is possible to study the virtually pristine LS state even in the SOXIESST regime provided that the X-ray flux is low enough. After irradiation with a significantly larger X-ray dose of D = 144 ph nm^{-2}, a high-spin fraction of 77 ± 3% (Figure 1b) was observed. The SOXIESST is fully reversible, as evidenced by the recovered LS state observed at 100 K after warming up to room temperature (Figure 1b). The magnetic moment of the LS state and the one of the HS state induced by SOXIESST were probed using X-ray magnetic circular dichroism at 3 K under an applied magnetic field of 6.8 T (Figure S2 and Table S1).

After these quasi-static investigations, we now follow the SOXIESST with a time resolution of 20 s by measuring the intensity of the X-ray absorption spectra at distinct energies only. The high-spin fraction is calculated from the HS (E_{HS} = 708.2 eV) and LS (E_{LS} = 709.5 eV) signals normalized to the pre-edge signal. The obtained HS fraction $\lambda(t)$ as a function of time, recorded at 3 K using a photon flux of ϕ_0 = 0.14 ph s^{-1} nm^{-2}, is displayed in Figure 1c. The HS fraction $\lambda(t)$ was fitted with the exponential function $\lambda(t) = \lambda^{\infty} - (\lambda^{\infty} - \lambda^{0})e^{-t/\tau}$, where τ = 360 ± 15 s is the time constant, λ^{∞} = 73 ± 7% is the HS fraction in saturation, and λ^{0} = 0% is the initial HS fraction at t = 0. Knowing the photon flux, the time constant can be converted into a cross section $\sigma_{pow} = \tau^{-1}\phi^{-1}$ = (1.96 ± 0.08) × 10^{-2} nm^{-2} = 196 ± 8 Mbarn, with 1 barn = 10^{-10} nm^2. This value is of the same order of magnitude as the SOXIESST cross section (600 Mbarn) of a submonolayer coverage of the SCO complex adsorbed on highly oriented pyrolytic graphite.[29] The difference of a factor of 3 is likely due to the different environments of the SCO complexes, i.e., monolayer coverage vs powder form. Interestingly, its value is ∼30 times larger than the cross section of the Fe L_3 absorption edge (σ_{XAS} ∼ 7 Mbarn).[32] This demonstrates that SOXIESST,[29] like hard X-ray-induced ESST[14] and vacuum-ultraviolet light-induced ESST,[15] is not directly caused by the X-ray absorption process. As suggested in refs 14 and 29 SOXIESST is likely due to scattering[33−35] of the large number of secondary electrons produced after the absorption of a single X-ray photon by the SCO molecules.

Interestingly, the value of the saturation HS fraction λ^{∞} = 73 ± 7% is comparable to the branching ratio at the $^3T_1$ triplet state during the initial fast relaxation after excitation into the HS or LS state, i.e., ∼4:1 in favor of the HS state.[29,36] λ^{∞} also agrees well with the HS fraction of λ = 77% (Figure 1b) found after irradiation with an X-ray dose of D = 144 ph nm^{-2}.

It is important to distinguish the reversible SOXIESST effect from the irreversible soft X-ray photochemistry (SOXPC), i.e., X-ray-induced degradation.[12] To determine the SOXPC rate, we have performed a separate experiment at 100 K, where SOXIESST is not observed. The SCO powder has been irradiated with a very high photon dose, D = 550 ph nm^{-2} (Figure 2). The spectra evidence a shoulder at lower energy corresponding to λ = 0.10. We estimate the photon cross section of SOXPC to be σ_{SOXPC} ∼ 2 Mbarn, a value which is ∼100 times smaller than the cross section for the reversible SOXIESST process, but nevertheless comparable to the absorption cross section of the Fe L_3 edge. The appearance of the HS signature at this temperature indicates that the molecules are irreversibly modified after the absorption of statistically around one X-ray photon.

Soft X-ray-Induced Spin-State Trapping of Molecular Thin Films on Ferroelectric Substrates. Molecular thin films of ∼70 nm thickness were grown on the (+)- and (−)-poled ferroelectric PMN-PT substrates as described in the Experimental Methods and Materials section. Figure 3 shows the X-ray absorption spectra of the thin films on both substrates at 300 and 100 K, respectively. At 300 K, 94 and 93% of the molecules are found in the HS state on (−)- and (+)-PMN-PT, respectively. The XAS line shapes of 70 nm and nominally 7 nm thin layers on differently poled PMN-PT substrates are virtually identical (Figure S3). At 100 K, the HS fraction is reduced to 33 and 24% on (−)- and (+)-PMN-PT, respectively. This indicates that the thermal SCO in both thin-film samples is less efficient than in the powder. Notably, also the thin films (∼80 and 8 nm nominal thicknesses) on polycrystalline gold prepared under the same conditions exhibit incomplete HS → LS conversion (Figure S4). This incomplete HS → LS conversion may be rationalized by a modified crystal packing or intercalation of, e.g., water molecules. A similar effect has been observed in other SCO thin films[18,37] as well as in SCO

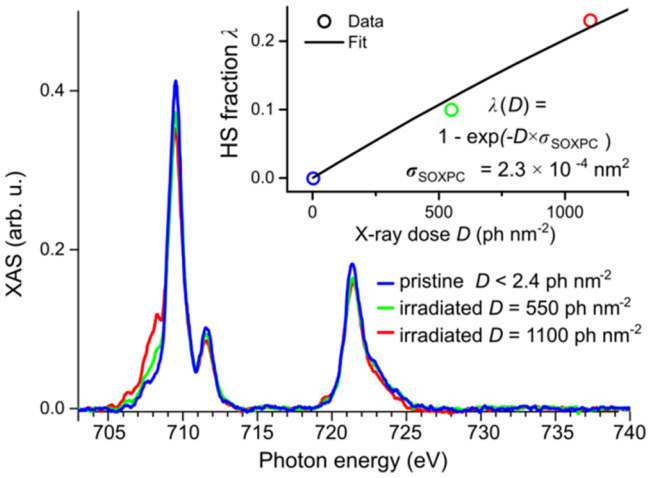

Figure 2. X-ray absorption spectra at the Fe $L_{2,3}$ edges recorded on the powder sample after irradiation with different photon doses at 100 K. Irradiation with a very high X-ray dose results in the appearance of a shoulder at low photon energy. Assuming that only the molecules that contribute to the shoulder are irreversibly modified, we estimate the photon cross section of SOXPC σ_{SOXPC} ∼ 2 Mbarn. Inset: HS fraction extracted from the spectra in the main panel as a function of photon dose.

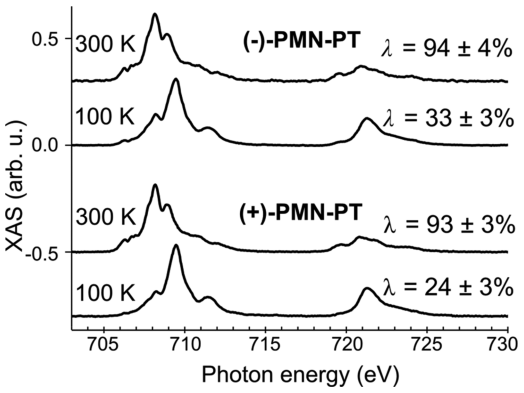

Figure 3. Temperature-dependent X-ray absorption spectra recorded on ∼70 nm thick molecular films on (+)- and (−)-polarized ferroelectric PMN-PT substrates. The molecules are predominantly in the HS state at 300 K and in the LS state at 100 K. The spectra have been offset for clarity.

DOI: 10.1021/acs.jpcc.7b10941
J. Phys. Chem. C 2018, 122, 8202−8208

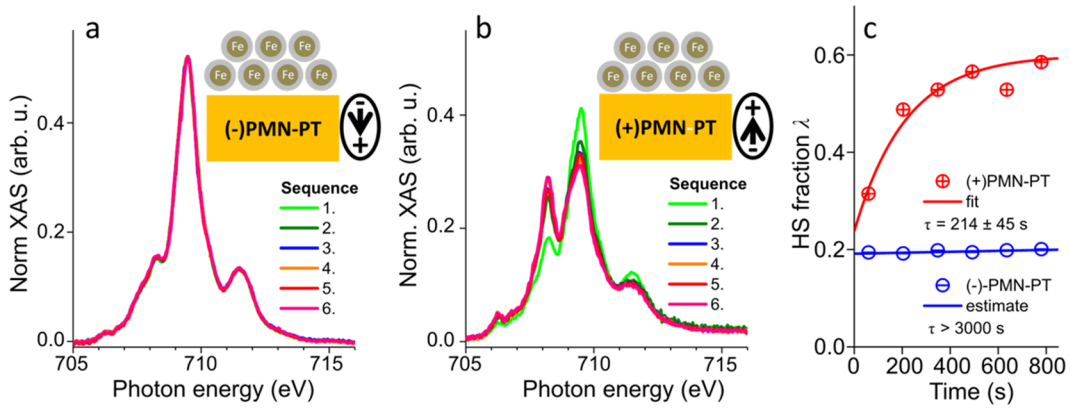

Figure 4. X-ray absorption spectra of thin films at 3 K on (+)- and (−)-polarized ferroelectric PMN-PT. (a, b) Sequence of six spectra on both substrates showing the Fe L_3 edge. At $\phi_0 = 0.14$ ph s^{-1} nm^{-2}, each spectrum corresponds to an X-ray dose of $D = 20$ ph nm^{-2}. Spin-state trapping is observed on (+)-PMN-PT, but not on (−)-PMN-PT. The spectra have been normalized to the same Fe L_3 peak area for visibility. (c) Time-dependent HS fractions extracted from the spectra shown in (a) and (b).

monolayers on graphite.[28] We note that deliberate intercalation of other molecules can lead to "locking" of the spin states.[38] The origin of the different HS fractions on (+)- and (−)-polarized PMN-PT and on gold at 100 K could be related to the adsorption of different small amounts of contaminants (e.g., water) on the differently polarized substrates on these ex situ samples[21,39] or to the observations reported in ref 24, where a complete suppression of the thermal (HS → LS) SCO down to 100 K was reported for one of the two polarizations of an organic ferroelectric thin film.

Next, we discuss SOXIESST in the thin film samples at 3 K, i.e., below T_{LIESST}, where also SOXIESST can occur. Figure 4a,b displays two sequences of six X-ray absorption spectra each on (−)- and (+)-PMN-PT, respectively. At the used photon flux $\phi_0 = 0.14$ ph s^{-1} nm^{-2}, each spectrum has an acquisition time t = 144 s, resulting in a dose of 20 ph nm^{-2}. Remarkably, we observe virtually no SOXIESST on the (−) poled substrate, whereas on the (+) poled sample, a significant HS fraction appears within minutes of irradiation. This is also seen in the extracted HS fractions (Figure 4c). This effect is also observed in similar experiments performed on thinner films (nominal thickness, 7 nm; Figure S5), but the initial HS fraction at 3 K is slightly higher, presumably due to more pronounced pinning of the SCO molecules.[38]

The SOXIESST rates $\tau^{-1}(\phi)$ recorded as a function of the X-ray flux ϕ are shown in Figure 5. The figure combines the rates obtained from the spectra with measurements at discrete energies. Both methods yield consistent values within the error. The data confirm that the rates for SOXIESST on the differently polarized substrates are both proportional to the X-ray flux. The corresponding values for the ESST cross sections $\sigma = \tau^{-1}\phi^{-1}$ on the different samples are listed in Table 1. We emphasize that the cross section $\sigma_{(+)}$ is similar to the one in the powder, whereas the cross section $\sigma_{(-)}$ is more than 1 order of magnitude lower. This is in accordance with the different time evolutions of the X-ray absorption spectra shown in Figure 4. Because the cross section for irreversible SOXPC is around 2 Mbarn, i.e., 6 times lower than the lowest observed SOXIESST cross section, its contribution to the reported cross sections remains within the error bars. The striking difference between the SOXIESST cross sections is another strong evidence that the SOXIESST mechanism is more complicated than simply the absorption of an X-ray photon and the subsequent deexcitation of the Fe(II) ion.

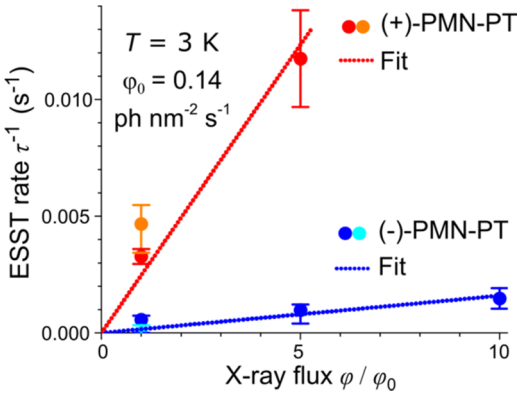

Figure 5. Comparison of flux-dependent ESST rates $\tau^{-1}(\phi)$. The dashed lines denote linear fits $\sigma = \tau^{-1}\phi^{-1}$ to the data. The resulting ESST cross sections σ are reported in Table 1. The orange and light blue data points correspond to the rate constants obtained from the sequences of spectra (Figure 4). The red and blue data points have been obtained by measuring X-ray absorption spectra at discrete energies.

Table 1. Excited Spin-State Trapping Cross Sections σ at 3 K for $[Fe(H_2B(pz)_2)_2(bipy)]$ SCO Complexes in Powder Form as Well as for Thin Films on the Ferroelectric Substrates

sample	σ (Mbarn)
SCO powder	196 ± 8
SCO on (+)-PMN-PT	174 ± 22
SCO on (−)-PMN-PT	12 ± 2

To shed light on the surprising difference in the ESST cross sections of the SCO thin films on the (+)- and (−)-polarized PMN-PT, we have analyzed the sequences of X-ray spectra obtained at 300 and 3 K (Figure 4a,b), each of which has been taken on fresh spots on the surface. X-ray illumination commenced at $t = 0$. Figure 6a displays the time-dependent intensity of the pre-edge TEY signals obtained at a photon energy of 704 eV from the X-ray spectra. A signal of 1 arb. unit in Figure 6a on the ordinate corresponds to ~0.4 nA of TEY current from the sample. Compared to 300 K, the TEY is significantly reduced at 3 K in both samples and a strong decay in time is observed. Remarkably, at low temperature, there is a sizeable difference between the signals from the (+)- and

DOI: 10.1021/acs.jpcc.7b10941
J. Phys. Chem. C 2018, 122, 8202−8208

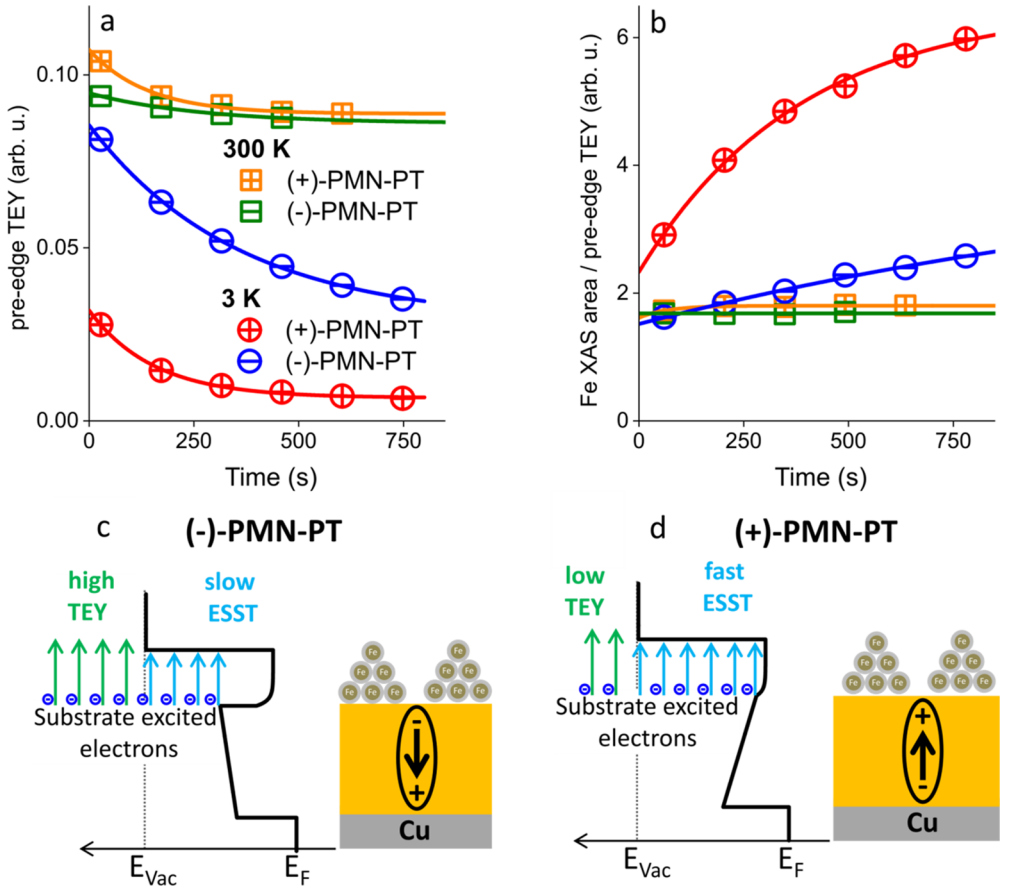

Figure 6. Data extracted from sequences of X-ray spectra of the SCO thin films on (+)- and (−)-PMN-PT at 300 and 3 K. (a) Time-dependent pre-edge TEY obtained at a photon energy of 704 eV. (b) Time-dependent integrated area of the Fe $L_{2,3}$ peaks normalized by the pre-edge TEY shown in (a). (c, d) Sketches of the lower conduction band edge of the (+)- and (−)-polarized PMN-PT substrates at low temperature, neglecting interface dipole effects. The green (blue) arrows denote X-ray-excited substrate electrons with sufficient (insufficient) kinetic energy to leave the sample. A higher rate of electrons remaining in the sample results in a higher SOXIESST rate.

(−)-poled substrates, which will be discussed further below. The integral of the Fe $L_{2,3}$ peaks divided by the pre-edge signal is shown in Figure 6b. An increase over time is observed at low temperature, which is more pronounced for the (+)-poled substrate.

The data shown in Figure 6a,b reveal a different behavior of the Fe XAS and the one of the pre-edge. While the Fe signal originates from the molecules, the pre-edge signal has contributions from the molecular ligand as well as from the substrate. The contribution of the latter depends on the exact sample morphology because the XAS probing depth is given by the electron escape depth of a few nanometers. Because the molecular ligand is unlikely to show charging different from the Fe(II) center ion, we deduce that the pre-edge TEY contains a significant amount of substrate electrons, which can be easily understood by the presence of empty surface areas related to the frequently observed inhomogeneous molecular island (Volmer−Weber) growth.

We attribute the time-dependent decrease of the pre-edge signal (Figure 6a) to charge depletion, which is commonly observed on insulating substrates under X-ray irradiation[40] because of the removal of electrons from the surface. The charging leads to an increase of the electron affinity and thus reduces the efficiency of extracting electrons from the substrate surface. The strength of the charging is given by the different, typically low, conductivities across the molecular deposit as well as through the substrate, which depend on temperature and ferroelectric polarization.[41] We note that during the X-ray measurements the TEY current density is extremely low (∼100 pA mm^{-2}). The small current only allows building up small electric fields across the substrate far from the ferroelectric poling threshold.

The energy band schemes of the two samples for the low-temperature case are shown in Figure 6c,d. The two different ferroelectric polarizations result in electric fields of opposite signs across the substrate, leading to different electron affinities at the surface.[39,42,43] Secondary electrons, which are generated in the substrate near the surface, are subjected to a larger electron affinity in the case of (+)-PMN-PT compared to (−)-PMN-PT, which results in the lower pre-edge signal observed in Figure 6a. This already happens at $t = 0$, when charging effects are not yet effective.

In the TEY mode used in this study, the signal corresponds directly to the total number of photo-, secondary-, and Auger-electrons.[44,45] Only the electrons with kinetic energy large enough to overcome the electron affinity leave the sample and contribute to the signal. In the case of large electron affinity, there are less electrons, which have sufficient energy to leave the sample, resulting in a lower TEY.[45] Therefore, a larger number of excited electrons remain in the sample and scatter with the molecules, resulting in a faster ESST on (+)-PMN-PT. We note that in this discussion interface dipole effects have

DOI: 10.1021/acs.jpcc.7b10941
J. Phys. Chem. C 2018, 122, 8202−8208

been neglected, which may lead to deviations of the band structures from the ones shown in Figure 6c,d. However, because of the low charge carrier densities of the molecules and the PMN-PT, this will mainly affect the Cu/PMN-PT interface at the back, which is irrelevant for the present results and their interpretation.

The X-ray-induced depletion of surface electrons discussed before leads to an increase of the electron affinity of the substrate disregarding its ferroelectric polarization. Hence, it enhances the contribution of ESST-active electrons. However, we emphasize that the dependence on the ferroelectric polarization is already visible at $t = 0$ before the charging effects set in.

The cross sections for the SOXIESST effect found in our study show that the spin multiplicity ($S = 0$ vs $S = 2$) of the SCO complex $[Fe(H_2B(pz)_2)_2(bipy)]$ is very sensitive to X-ray radiation. The effect works through scattering of excited electrons, as evident from the fact that its cross section is much higher than the Fe L_3 X-ray absorption cross section. In this regard, SOXIESST bears some analogy with X-ray-induced demagnetization,[33−35] which affects the magnetic moments of single-molecule magnets.

CONCLUSIONS

We have performed an XAS study of SCO thin films deposited on ferroelectric PMN-PT. In the SOXIESST regime, the ferroelectric polarization has a strong influence on the X-ray-induced LS-to-HS conversion rate; hence, the cross section for SOXIESST can be tuned by more than 1 order of magnitude by switching the ferroelectric polarization. The reason behind this large difference is given by the different electron affinities of the two differently poled substrates. Furthermore, we have characterized the cross section for the SOXIESST effect as well as the one for X-ray photochemistry. The large SOXIESST cross sections indicate that one X-ray photon results in the promotion of many SCO molecules to the HS state, suggesting that the mechanism proceeds through scattering of excited secondary electrons. We anticipate that the efficiency of spin-state trapping via scattering with electrons can be tuned by gating the electric field. SCO complexes may also be useful as sensors for ionizing radiation and for the detection of excited electrons with energies lower than the electron affinity traveling within materials.

ASSOCIATED CONTENT

Supporting Information

The Supporting Information is available free of charge on the ACS Publications website at DOI: 10.1021/acs.jpcc.7b10941.

Voltage-dependent displacement current during the poling process of the PMN-PT substrate, XAS and X-ray magnetic circular dichroism images of the complex after exposure to low and high photon doses, sum rule analysis, XAS image of the complex deposited on polycrystalline gold, X-ray absorption spectra evidencing SOXIESST in thinner films on PMN-PT (PDF)

AUTHOR INFORMATION

Corresponding Authors

*E-mail: christian.waeckerlin@empa.ch (C.W.).
*E-mail: jan.dreiser@psi.ch (J.D.).

ORCID

Christian Wäckerlin: 0000-0001-6587-1235
Stefano Rusponi: 0000-0002-8494-5532
Jan Dreiser: 0000-0001-7480-1271

Notes

The authors declare no competing financial interest.

ACKNOWLEDGMENTS

J.D. and C.W. gratefully acknowledge funding from the Swiss National Science Foundation (grant no. PZ00P2_142474). C.W. acknowledges financial support from the University of Zurich priority program LightChEC. F.D. acknowledges support from IBSR027-D1. The authors thank Stephan Keller for assistance with the synthesis. Also, they thank Cinthia Piamonteze and Jakoba Heidler for assistance with the ferroelectric poling setup.

REFERENCES

(1) Létard, J.-F.; Guionneau, P.; Goux-Capes, L. Towards Spin Crossover Applications. *Spin Crossover in Transition Metal Compounds III*; Springer-Verlag: Berlin, 2004; Vol. *235*, pp 221−249.

(2) Prins, F.; Monrabal-Capilla, M.; Osorio, E. A.; Coronado, E.; van der Zant, H. S. J. Room-Temperature Electrical Addressing of a Bistable Spin-Crossover Molecular System. *Adv. Mater.* **2011**, *23*, 1545−1549.

(3) Pointillart, F.; Liu, X.; Kepenekian, M.; Le Guennic, B.; Golhen, S.; Dorcet, V.; Roisnel, T.; Cador, O.; You, Z.; Hauser, J.; et al. Thermal and Near-Infrared Light Induced Spin Crossover in a Mononuclear Iron(II) Complex with a Tetrathiafulvalene-Fused Dipyridophenazine Ligand. *Dalton Trans.* **2016**, *45*, 11267−11271.

(4) Letard, J. F.; Guionneau, P.; Goux-Capes, L. *Spin Crossover in Transition Metal Compounds*; Topics in Current Chemistry; Springer: Berlin, 2004.

(5) Gütlich, P. Nuclear Decay Induced Excited Spin State Trapping (NIESST). *Spin Crossover in Transition Metal Compounds II*; Springer: Berlin, 2004; Vol. *234*, pp 231−260.

(6) Decurtins, S.; Gütlich, P.; Köhler, C. P.; Spiering, H.; Hauser, A. Light-Induced Excited Spin State Trapping in a Transition-Metal Complex: The Hexa-1-Propyltetrazole-Iron (II) Tetrafluoroborate Spin-Crossover System. *Chem. Phys. Lett.* **1984**, *105*, 1−4.

(7) Decurtins, S.; Gütlich, P.; Hasselbach, K. M.; Hauser, A.; Spiering, H. Light-Induced Excited-Spin-State Trapping in Iron(II) Spin-Crossover Systems. Optical Spectroscopic and Magnetic Susceptibility Study. *Inorg. Chem.* **1985**, *24*, 2174−2178.

(8) Decurtins, S.; Gütlich, P.; Köhler, C. P.; Spiering, H. New Examples of Light-Induced Excited Spin State Trapping (LIESST) in Iron(II) Spin-Crossover Systems. *J. Chem. Soc., Chem. Commun.* **1985**, 430−432.

(9) Sano, H.; Gütlich, P. Hot Atom Chemistry in Relation to Mossbauer Emission Spectroscopy. In *Hot Atom Chemistry*; Matsuura, T., Ed.; Kodanski: Tokyo, 1984; p 265.

(10) Gopakumar, T. G.; Matino, F.; Naggert, H.; Bannwarth, A.; Tuczek, F.; Berndt, R. Electron-Induced Spin Crossover of Single Molecules in a Bilayer on Gold. *Angew. Chem., Int. Ed.* **2012**, *51*, 6262−6266.

(11) Gopakumar, T. G.; Bernien, M.; Naggert, H.; Matino, F.; Hermanns, C. F.; Bannwarth, A.; Mühlenberend, S.; Krüger, A.; Krüger, D.; Nickel, F.; et al. Spin-Crossover Complex on Au(111): Structural and Electronic Differences Between Mono- and Multilayers. *Chem. - Eur. J.* **2013**, *19*, 15702−15709.

(12) Collison, D.; Garner, C. D.; McGrath, C. M.; Mosselmans, J. F. W.; Roper, M. D.; Seddon, J. M. W.; Sinn, E.; Young, N. A. Soft X-Ray Induced Excited Spin State Trapping and Soft X-Ray Photochemistry at the Iron $L_{2,3}$ Edge in $[Fe(phen)_2(NCS)_2]$ and $[Fe(phen)_2(NCSe)_2]$ (phen = 1,10-phenanthroline). *J. Chem. Soc., Dalton Trans.* **1997**, 4371−4376.

(13) Davesne, V.; Gruber, M.; Miyamachi, T.; Da Costa, V.; Boukari, S.; Scheurer, F.; Joly, L.; Ohresser, P.; Otero, E.; Choueikani, F.; et al. First Glimpse of the Soft X-Ray Induced Excited Spin-State Trapping

DOI: 10.1021/acs.jpcc.7b10941
J. Phys. Chem. C 2018, 122, 8202−8208

Effect Dynamics on Spin Cross-over Molecules. *J. Chem. Phys.* **2013**, *139*, No. 074708.
(14) Vankó, G.; Renz, F.; Molnár, G.; Neisius, T.; Kárpáti, S. Hard-X-Ray-Induced Excited-Spin-State Trapping. *Angew. Chem., Int. Ed.* **2007**, *46*, 5306−5309.
(15) Ludwig, E.; Naggert, H.; Kalläne, M.; Rohlf, S.; Kröger, E.; Bannwarth, A.; Quer, A.; Rossnagel, K.; Kipp, L.; Tuczek, F. Iron(II) Spin-Crossover Complexes in Ultrathin Films: Electronic Structure and Spin-State Switching by Visible and Vacuum-UV Light. *Angew. Chem., Int. Ed.* **2014**, *53*, 3019−3023.
(16) Cartier dit Moulin, C.; Rudolf, P.; Flank, A. M.; Chen, C. T. Spin Transition Evidenced by Soft X-Ray Absorption Spectroscopy. *J. Phys. Chem.* **1992**, *96*, 6196−6198.
(17) Real, J. A.; Muñoz, M. C.; Faus, J.; Solans, X. Spin Crossover in Novel Dihydrobis(1-pyrazolyl)borate $[H_2B(pz)_2]$-Containing Iron(II) Complexes. Synthesis, X-Ray Structure, and Magnetic Properties of $[FeL\{H_2B(pz)_2\}_2]$ (L = 1,10-phenanthroline and 2,2′-bipyridine). *Inorg. Chem.* **1997**, *36*, 3008−3013.
(18) Naggert, H.; Bannwarth, A.; Chemnitz, S.; von Hofe, T.; Quandt, E.; Tuczek, F. First Observation of Light-Induced Spin Change in Vacuum Deposited Thin Films of Iron Spin Crossover Complexes. *Dalton Trans.* **2011**, *40*, 6364−6366.
(19) Yin, Z.-W.; Luo, H.-S.; Wang, P.-C.; Xu, G.-S. Growth, Characterization and Properties of Relaxor Ferroelectric PMN-PT Single Crystals. *Ferroelectrics* **1999**, *229*, 207−216.
(20) Wu, T.; Zhao, P.; Bao, M.; Bur, A.; Hockel, J. L.; Wong, K.; Mohanchandra, K. P.; Lynch, C. S.; Carman, G. P. Domain Engineered Switchable Strain States in Ferroelectric (011) $[Pb(Mg_{1/3}Nb_{2/3})O_3]_{(1-x)}$-$[PbTiO_3]_x$(PMN-PT, x ≈ 0.32) Single Crystals. *J. Appl. Phys.* **2011**, *109*, No. 124101.
(21) Zhang, Z.; González, R.; Díaz, G.; Rosa, L. G.; Ketsman, I.; Zhang, X.; Sharma, P.; Gruverman, A.; Dowben, P. A. Polarization Mediated Chemistry on Ferroelectric Polymer Surfaces. *J. Phys. Chem. C* **2011**, *115*, 13041−13046.
(22) Dowben, P. A.; Rosa, L. G.; Ilie, C. C.; Xiao, J. Adsorbate/Absorbate Interactions with Organic Ferroelectric Polymers. *J. Electron Spectrosc. Relat. Phenom.* **2009**, *174*, 10−21.
(23) Zhang, Z.; Sharma, P.; Borca, C. N.; Dowben, P. A.; Gruverman, A. Polarization-Specific Adsorption of Organic Molecules on Ferroelectric $LiNbO_3$ Surfaces. *Appl. Phys. Lett.* **2010**, *97*, No. 243702.
(24) Zhang, X.; Palamarciuc, T.; Létard, J.-F.; Rosa, P.; Lozada, E. V.; Torres, F.; Rosa, L. G.; Doudin, B.; Dowben, P. A. The Spin State of a Molecular Adsorbate Driven by the Ferroelectric Substrate Polarization. *Chem. Commun.* **2014**, *50*, 2255−2257.
(25) Heidler, J.; Piamonteze, C.; Chopdekar, R. V.; Uribe-Laverde, M. A.; Alberca, A.; Buzzi, M.; Uldry, A.; Delley, B.; Bernhard, C.; Nolting, F. Manipulating Magnetism in $La_{0.7}Sr_{0.3}MnO_3$ via Piezostrain. *Phys. Rev. B* **2015**, *91*.10.1103/PhysRevB.91.024406.
(26) Heidler, J. Ferroelectric Control of Magnetism in Articial Multiferroic Composites. Ph.D. Dissertation, University of Basel, 2015.
(27) Piamonteze, C.; Flechsig, U.; Rusponi, S.; Dreiser, J.; Heidler, J.; Schmidt, M.; Wetter, R.; Calvi, M.; Schmidt, T.; Pruchova, H.; et al. X-Treme Beamline at SLS: X-Ray Magnetic Circular and Linear Dichroism at High Field and Low Temperature. *J. Synchrotron Radiat.* **2012**, *19*, 661−674.
(28) Bernien, M.; Wiedemann, D.; Hermanns, C. F.; Krüger, A.; Rolf, D.; Kroener, W.; Müller, P.; Grohmann, A.; Kuch, W. Spin Crossover in a Vacuum-Deposited Submonolayer of a Molecular Iron(II) Complex. *J. Phys. Chem. Lett.* **2012**, *3*, 3431−3434.
(29) Kipgen, L.; Bernien, M.; Nickel, F.; Naggert, H.; Britton, A. J.; Arruda, L. M.; Schierle, E.; Weschke, E.; Tuczek, F.; Kuch, W. Soft-x-Ray-Induced Spin-State Switching of an Adsorbed Fe(II) Spin-Crossover Complex. *J. Phys.: Condens. Matter* **2017**, *29*, No. 394003.
(30) Bernien, M.; Naggert, H.; Arruda, L. M.; Kipgen, L.; Nickel, F.; Miguel, J.; Hermanns, C. F.; Krüger, A.; Krüger, D.; Schierle, E.; et al. Highly Efficient Thermal and Light-Induced Spin-State Switching of an Fe(II) Complex in Direct Contact with a Solid Surface. *ACS Nano* **2015**, *9*, 8960−8966.
(31) Moliner, N.; Salmon, L.; Capes, L.; Muñoz, M. C.; Létard, J.-F.; Bousseksou, A.; Tuchagues, J.-P.; McGarvey, J. J.; Dennis, A. C.; Castro, M.; et al. Thermal and Optical Switching of Molecular Spin States in the $\{[FeL[H_2B(pz)_2]_2\}$ Spin-Crossover System (L = bpy, phen). *J. Phys. Chem. B* **2002**, *106*, 4276−4283.
(32) Regan, T.; Ohldag, H.; Stamm, C.; Nolting, F.; Lüning, J.; Stöhr, J.; White, R. Chemical Effects at Metal/Oxide Interfaces Studied by X-Ray-Absorption Spectroscopy. *Phys. Rev. B* **2001**, *64*, No. 214422.
(33) Dreiser, J.; Westerström, R.; Piamonteze, C.; Nolting, F.; Rusponi, S.; Brune, H.; Yang, S.; Popov, A.; Dunsch, L.; Greber, T. X-Ray Induced Demagnetization of Single-Molecule Magnets. *Appl. Phys. Lett.* **2014**, *105*, No. 032411.
(34) Wäckerlin, C.; Donati, F.; Singha, A.; Baltic, R.; Rusponi, S.; Diller, K.; Patthey, F.; Pivetta, M.; Lan, Y.; Klyatskaya, S.; et al. Giant Hysteresis of Single-Molecule Magnets Adsorbed on a Nonmagnetic Insulator. *Adv. Mater.* **2016**, *28*, 5195−5199.
(35) Donati, F.; Rusponi, S.; Stepanow, S.; Wäckerlin, C.; Singha, A.; Persichetti, L.; Baltic, R.; Diller, K.; Patthey, F.; Fernandes, E.; et al. Magnetic Remanence in Single Atoms. *Science* **2016**, *352*, 318−321.
(36) Hauser, A. Light-Induced Spin Crossover and the High-Spin → Low-Spin Relaxation. *Spin Crossover in Transition Metal Compounds II*; Springer: Berlin, 2004; Vol. *234*, pp 155−198.
(37) Palamarciuc, T.; Oberg, J. C.; El Hallak, F.; Hirjibehedin, C. F.; Serri, M.; Heutz, S.; Létard, J.-F.; Rosa, P. Spin Crossover Materials Evaporated under Clean High Vacuum and Ultra-High Vacuum Conditions: From Thin Films to Single Molecules. *J. Mater. Chem.* **2012**, *22*, 9690−9695.
(38) Zhang, X.; Costa, P. S.; Hooper, J.; Miller, D. P.; N'Diaye, A. T.; Beniwal, S.; Jiang, X.; Yin, Y.; Rosa, P.; Routaboul, L.; et al. Locking and Unlocking the Molecular Spin Crossover Transition. *Adv. Mater.* **2017**, *29*, No. 1702257.
(39) Wang, J. L.; Vilquin, B.; Barrett, N. Screening of Ferroelectric Domains on BaTiO3(001) Surface by Ultraviolet Photo-Induced Charge and Dissociative Water Adsorption. *Appl. Phys. Lett.* **2012**, *101*, No. 092902.
(40) Vlachos, D.; Craven, A. J.; McComb, D. W. Specimen Charging in X-Ray Absorption Spectroscopy: Correction of Total Electron Yield Data from Stabilized Zirconia in the Energy Range 250−915 eV. *J. Synchrotron Radiat.* **2005**, *12*, 224−233.
(41) Choi, T.; Lee, S.; Choi, Y. J.; Kiryukhin, V.; Cheong, S.-W. Switchable Ferroelectric Diode and Photovoltaic Effect in $BiFeO_3$. *Science* **2009**, *324*, 63−66.
(42) Yang, W.-C.; Rodriguez, B. J.; Gruverman, A.; Nemanich, R. J. Polarization-Dependent Electron Affinity of $LiNbO_3$ Surfaces. *Appl. Phys. Lett.* **2004**, *85*, 2316.
(43) Barrett, N.; Rault, J. E.; Wang, J. L.; Mathieu, C.; Locatelli, A.; Mentes, T. O.; Niño, M. A.; Fusil, S.; Bibes, M.; Barthélémy, A.; et al. Full Field Electron Spectromicroscopy Applied to Ferroelectric Materials. *J. Appl. Phys.* **2013**, *113*, No. 187217.
(44) Stöhr, J. *NEXAFS Spectroscopy*, 1st ed. corr. print.; Springer Series in Surface Sciences; Springer: Berlin, 1996.
(45) Henke, B.; Liesegang, J.; Smith, S. Soft-X-Ray-Induced Secondary-Electron Emission from Semiconductors and Insulators: Models and Measurements. *Phys. Rev. B* **1979**, *19*, 3004−3021.

DOI: 10.1021/acs.jpcc.7b10941
J. Phys. Chem. C 2018, 122, 8202−8208

Supporting Information

Excited Spin-State Trapping in Spin Crossover Complexes on Ferroelectric Substrates

Christian Wäckerlin[†,‡,], Fabio Donati[§,†,¥], Aparajita Singha[†], Romana Baltic[†], Silvio Decurtins[⊥], Shi-Xia Liu[⊥], Stefano Rusponi[†], Jan Dreiser[∥,*]*

[†]Institute of Physics, Ecole Polytechnique Fédérale de Lausanne, Station 3, 1015 Lausanne, Switzerland

[‡]Nanoscale Materials Science, Empa, Swiss Federal Laboratories for Materials Science and Technology, 8600 Dübendorf, Switzerland

[§] Center for Quantum Nanoscience, Institute for Basic Science (IBS), Seoul 03760, Republic of Korea

[¥] Department of Physics, Ewha Womans University, Seoul 03760, Republic of Korea

[⊥]Department of Chemistry and Biochemistry, University of Bern, Freiestrasse 3, 3012 Bern, Switzerland

[∥]Swiss Light Source, Paul Scherrer Institut, 5232 Villigen PSI, Switzerland

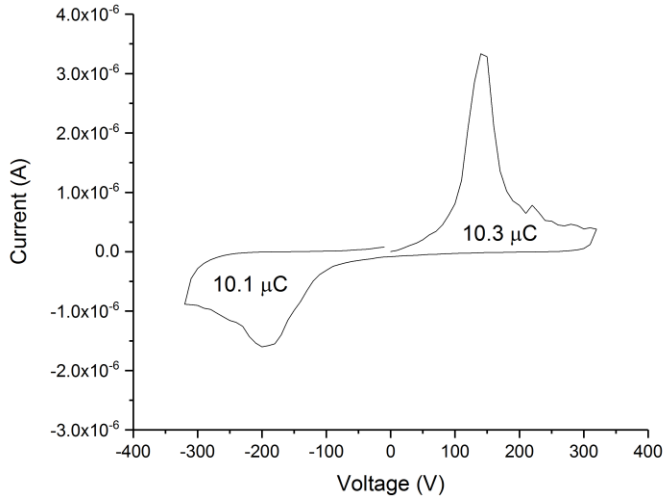

Figure S1 Typical voltage-dependent displacement current monitored during the poling process at a sweep rate of 30 V/s at room temperature. The sample size is 8 mm × 4 mm. The integrated displacement charge of 31.9 μC/cm^2 is consistent with the value of 32 μC/cm^2 reported in ref. 1 indicating that the ferroelectric poling is complete.

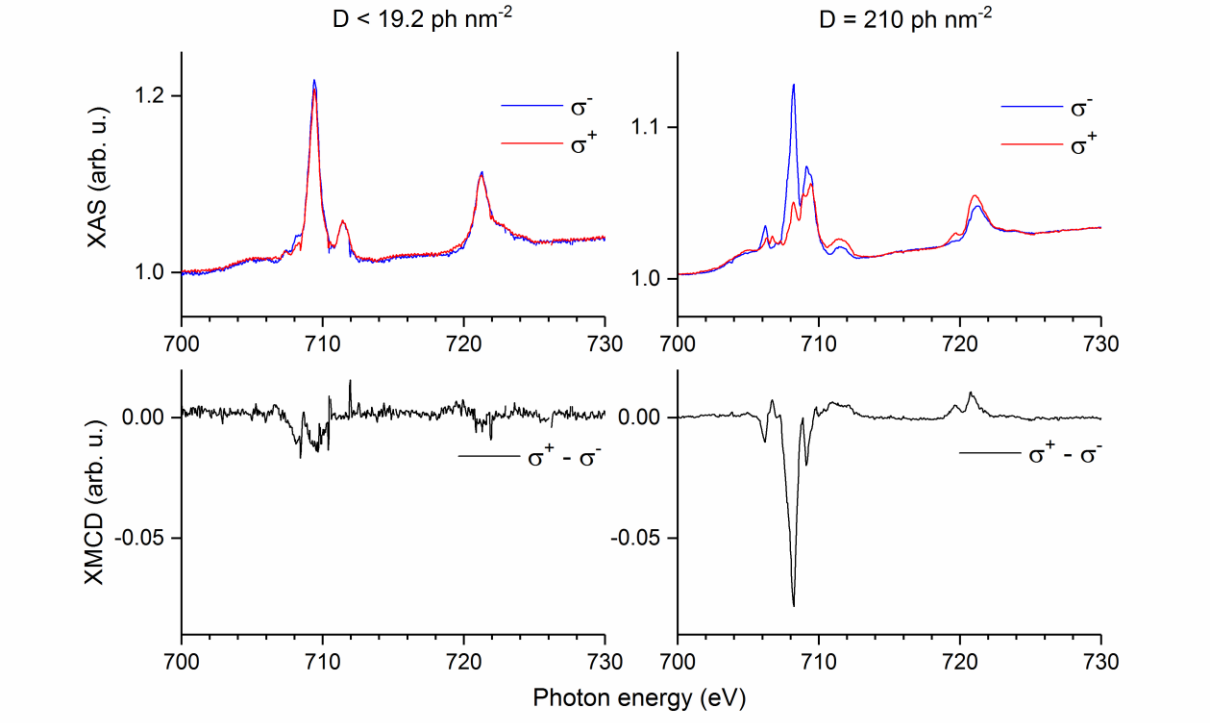

Figure S2 XAS and XMCD spectra recorded for the SCO complex in powder form at 3 K. At low photon irradiation doses, almost all molecules are in the low spin form. Only a small XMCD signal is observed, consistent

with the non-zero photon dose. After irradiation, a significant XMCD signal is observed, consistent with soft X-ray induced spin state trapping.

Table S1 Sum rule analysis of the spectra shown in Figure S2. The number of holes is assumed to be 4, appropriate for an Fe(II) complex. The high spin fraction λ is calculated from the ratio of the HS and LS peaks in the unpolarized XAS as described in the main text. The true spin angular momentum $\langle S_z \rangle$ may be slightly larger than the effective spin $\langle S_{eff} \rangle$ measured here, $\langle S_z \rangle = \langle S_{eff} \rangle / c$, where $c = (0.8 - 0.95)$.[2] Considering the HS fraction and the correction factor c, a total spin magnetic moment of $m_s = 2\langle S_z \rangle \mu_B$ of 2.6 to 3.1 μ_B is found for 100 % HS complexes.

Sample	$m_{s,eff,z}$	$m_{l,z}$	λ
D < 19.2 ph nm^{-2}	0.15 ± 0.05 μ_B	0.02 ± 0.05 μ_B	3 ± 3 %
D = 210 ph nm^{-2}	1.9 ± 0.2 μ_B	0.5 ± 0.1 μ_B	77 ± 3 %

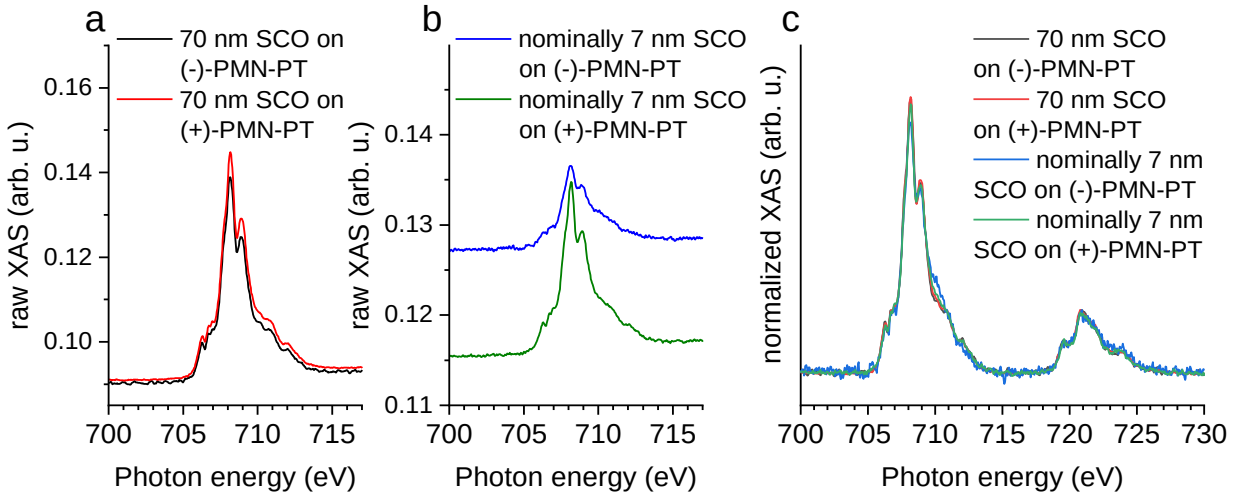

Figure S3 (a,b) Raw XAS recorded at 300 K at the Fe L_3 edge of the 70 nm and the nominally 7 nm SCO deposits on the differently poled substrates as indicated in the plots. The different strength of the Fe L_3 edge absorption in panel b) could be due to sticking coefficients varying for the ferroelectric polarizations,[3] which is less relevant for the thicker films in panel a). (c) Same as in (a,b) but showing Fe $L_{2,3}$ edges normalized with respect to the Fe L_3 edge. The spectral line-shapes are very similar indicating the presence of structurally intact molecules.

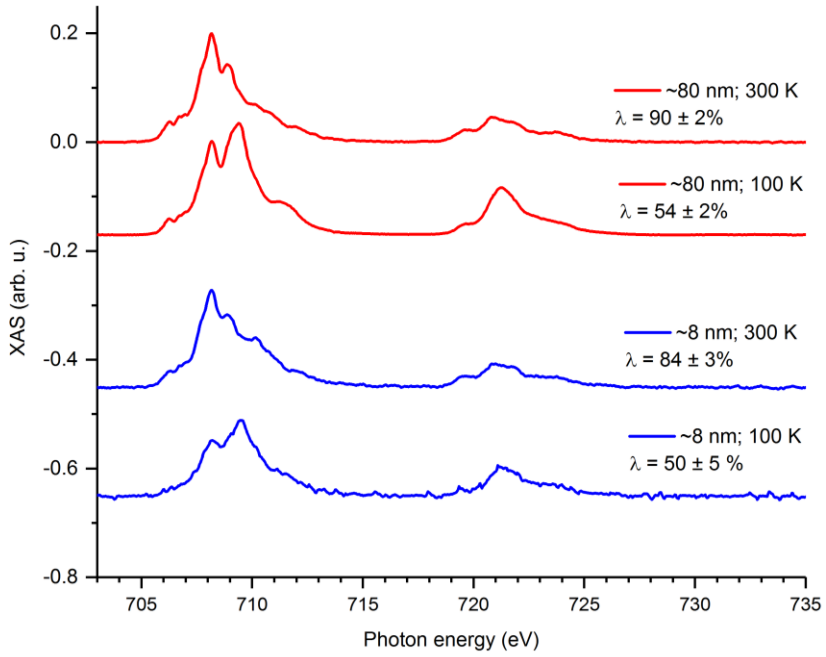

Figure S4 XAS of the SCO complex deposited on polycrystalline gold. Spectra were recorded at 300 K and at 100 K as indicated in the plots. The thicknesses of the films are calculated from the sublimation times.

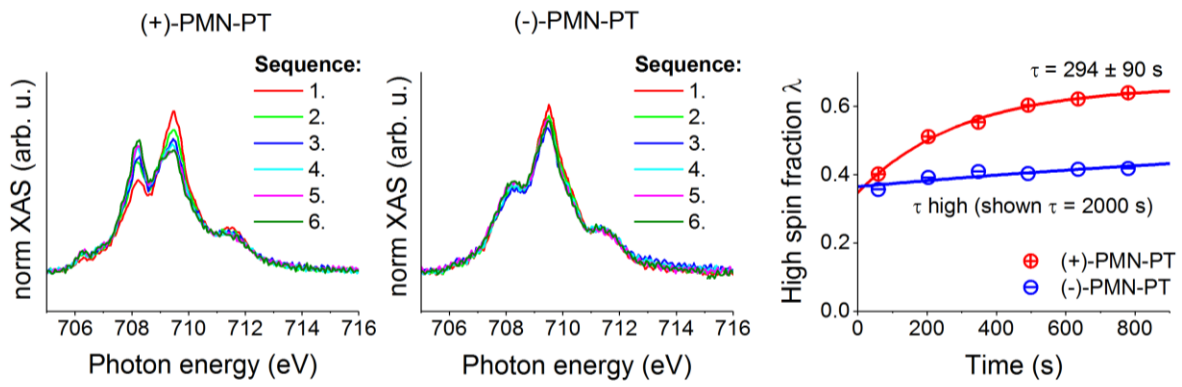

Figure S5 XAS of thin films with nominal thickness 7 nm at 3 K on (+) and (-) polarized ferroelectric PMN-PT. The nominal thickness is calculated from the sublimation time. Sequence of spectra on both substrates showing the Fe L_3 edge, respectively. Photon flux $\phi_0 = 0.14\ \mathrm{ph\ s^{-1}\ nm^{-2}}$, each spectrum corresponds to a X-ray dose of $D = 20\ \mathrm{ph\ nm^{-2}}$. The spectra have been normalized to the same Fe L_3 peak area for visibility. Time dependent HS fractions extracted from the spectra as shown. Spin-state trapping is observed on (+)-PMN-PT but not on (-)-PMN-PT.

REFERENCES

(1) Wu, T.; Zhao, P.; Bao, M.; Bur, A.; Hockel, J. L.; Wong, K.; Mohanchandra, K. P.; Lynch, C. S.; Carman, G. P. Domain Engineered Switchable Strain States in Ferroelectric (011) $[Pb(Mg_{1/3}Nb_{2/3})O_3]_{(1-x)}$-$[PbTiO_3]_x$(PMN-PT, x≈0.32) Single Crystals. *J. Appl. Phys.* **2011**, *109*, 124101.

(2) Piamonteze, C.; Miedema, P.; de Groot, F. M. F. Accuracy of the Spin Sum Rule in XMCD for the Transition-Metal L Edges from Manganese to Copper. *Phys. Rev. B* **2009**, *80*, 184410.

(3) Zhang, Z.; González, R.; Díaz, G.; Rosa, L. G.; Ketsman, I.; Zhang, X.; Sharma, P.; Gruverman, A.; Dowben, P. A. Polarization Mediated Chemistry on Ferroelectric Polymer Surfaces. *J. Phys. Chem. C* **2011**, *115*, 13041–13046.